Local Induction of Adiponectin Reduces Lipopolysaccharide-Triggered Skeletal Muscle Damage

Julie Jortay, Maximin Senou, Aurélie Delaigle, Laurence Noel, Tohru Funahashi, Norikazu Maeda, Marie C. Many, and Sonia M. Brichard

Endocrinology and Metabolism Unit (J.J., A.D., L.N., S.M.B.) and Experimental Morphology Unit (M.S., M.C.M.), Faculty of Medicine, University of Louvain, 1200 Brussels, Belgium; and Department of Internal Medicine and Molecular Science (T.F., N.M.), Graduate School of Medicine, Osaka University, Osaka 565-0871, Japan

Adiponectin (ApN) exhibits metabolic and antiinflammatory properties. This hormone is exclusively secreted by adipocytes under normal conditions. We have shown that ApN was induced in tibialis anterior muscle of mice injected with lipopolysaccharide (LPS) and in C2C12 myotubes cultured with proinflammatory cytokines. We hypothesized that muscle ApN could be a local protective mechanism to counteract excessive inflammatory reaction and oxidative damage. To test this paradigm, we examined whether muscles of ApN-knockout (KO) mice exhibit a higher degree of oxidative stress and apoptosis than wild-type mice when challenged by ip LPS and whether these abnormalities may be corrected by local administration of ApN. Eventually we investigated the effects of ApN *in vitro*. When compared with wild-type mice, ApN-KO mice exhibited myocyte degenerescence, especially after LPS. Myocytes of ApN-KO mice also displayed much stronger immunolabeling for markers of oxidative stress (peroxiredoxin-3/5 and heme oxygenase-1) as well as for a lipid peroxidation product (hydroxynonenal). Expression of TNF-α, caspase-6, a marker of apoptosis, and nuclear factor-κB was enhanced as well. Eventually muscle electrotransfer of the ApN gene, which did not induce any rise of systemic ApN, corrected all these abnormalities in LPS-injected ApN-KO mice. Likewise, ApN attenuated LPS-induced production of proinflammatory cytokines and activation of nuclear factor-κB in C2C12 cells. Thus, induction of ApN into skeletal muscle in response to an inflammatory aggression appears to be a crucial mechanism to counteract in an autocrine or paracrine fashion excessive inflammatory damage, oxidative stress, and subsequent apoptosis. **(*Endocrinology* 151: 4840–4851, 2010)**

Adiponectin (ApN) is a hormone abundantly secreted by the adipocytes. Unlike most other adipokines, circulating ApN is negatively correlated with body mass index and decreased in obese subjects and patients who meet criteria for the metabolic syndrome (1). A number of experimental studies suggest that ApN can exhibit insulin-sensitizing, fat-burning, and antiinflammatory properties as well as a modulatory effect on oxidative stress, thereby thwarting simultaneously several facets of the metabolic syndrome (2, 3).

ApN receptor (AdipoR)-1 and AdipoR2 serve as major receptors for ApN *in vivo* (4). AdipoR1 is abundantly expressed in muscle, whereas AdipoR2 is also expressed in liver (5). The molecular mechanism by which ApN mediates enhanced insulin sensitivity is mainly linked to increased glucose uptake and fatty acid oxidation and decreased gluconeogenesis via activation of AMP-activated protein kinase, peroxisomal proliferator-activated receptor-α, and p38 MAPK (6). ApN also attenuates inflammatory and oxidative responses to multiple stimuli by

ISSN Print 0013-7227 ISSN Online 1945-7170
Printed in U.S.A.

doi: 10.1210/en.2009-1462 Received December 16, 2009. Accepted July 9, 2010.
First Published Online August 11, 2010

Abbreviations: AdipoR, ApN receptor; ApN, adiponectin; Ct, threshold cycle; HES, hematoxylin-eosin-safran; HNE, 4-hydroxy-2-nonenal; HO-1, heme oxygenase 1; IκB, inhibitory-κB; KO, knockout; LPS, lipopolysaccharide; NEFA, nonesterified fatty acid; NF-κB, nuclear factor-κB; PRDX, peroxiredoxin; RTQ-PCR, real-time quantitative PCR; TBARS, thiobarbituric acid reactive substance; WT, wild-type.

modulating different signaling pathways in a variety of cell types (for review see Ref. 1). In this respect, endothelial cells have been the most studied. ApN has been shown to inhibit TNF-α-induced activation of nuclear factor-κB (NF-κB) and suppress superoxide radical generation in these cells (7, 8). The antiinflammatory and antioxidative properties of ApN may play a major role in its beneficial effects on cardiovascular and metabolic disorders such as atherosclerosis and insulin resistance (1, 9).

Skeletal muscle has been recognized as an endocrine organ that produces and releases biologically active cytokines/hormones, belonging to distinctly different families, collectively referred to as myokines (10). Although ApN is exclusively secreted by the adipocyte under normal conditions, emerging studies point out its presence in nonadipose tissues (11), such as skeletal muscle (12–17), in which the adipokine has been detected within myofibers (13, 15).

We have shown that ApN may be induced in skeletal muscle after an inflammatory aggression (12) or a metabolic and oxidative stress, like that occurring in type 2 diabetes (13). Thus, ApN was up-regulated in tibialis anterior muscle of mice injected with lipopolysaccharide (LPS) and in C2C12 myotubes cultured in the presence of proinflammatory cytokines (12). We have speculated that this induction of ApN could be a local protective mechanism, which is needed to counterbalance inflammatory aggression in muscle.

The aim of the present work was to test this hypothesis. To this end, we first examined *in vivo* whether muscles of ApN-deficient mice exhibit higher degree of oxidative stress and apoptosis than those of wild-type mice when challenged by LPS and whether these abnormalities may be corrected by local administration of ApN. Next, we examined *in vitro* the effect of ApN on cytokine production by C2C12 myotubes challenged with LPS.

Materials and Methods

Animals

ApN-knockout (KO) mice, which are characterized by a generalized lack of ApN, were obtained from Maeda *et al.* (18) and maintained on a C57BL6/J background. Wild-type (WT) controls were C57BL/6J mice that were raised together with KO mice (but were not their littermates). Male KO and WT mice were housed at a constant temperature (22 C) with a fixed 12-h light, 12-h dark cycle. These animals received *ad libitum* a standard diet (Rat and Mouse no. 3 Breeding; Specials Diets Services, Witham, UK) and were studied at the age of 12 wk.

LPS of *Escherichia coli* (serotype 0127:B8; Sigma-Aldrich, Bornem, Belgium) was dissolved in saline at a concentration of 0.4 mg/ml. At 0900 h, mice were injected ip with 250 μl LPS (100 μg/animal) or equivalent volume of saline. Four groups of mice were studied: untreated WT (receiving saline), untreated ApN-KO (receiving saline), LPS-treated WT, and LPS-treated ApN-KO mice. Because LPS-injected mice reduced their daily food intake by 95% in our preliminary experiments, all groups of mice were fasted after the injection (saline/LPS). Mice were killed by decapitation (between 0900 and 1030 h) 24 h later. Blood samples were saved. Pairs of tibialis anterior muscles and inguinal fat were dissected, weighed, frozen in liquid nitrogen, and stored at −80 C. In some mice, blood was also collected 0, 1, and 3 h after LPS injection.

In an additional experiment, ApN-KO mice were submitted to muscle electrotransfer of the *ApN* gene. Animals were anesthetized with a mixture of ketamine (75 mg/kg body weight; Ketalar, Pfizer, New York, NY) and xylazine hydrochloride (10 mg/kg body weight; Sigma-Aldrich) administered by ip injection. One tibialis anterior muscle was injected and electroporated by ApN cDNA containing-plasmid (left) and the contralateral muscle by an empty plasmid (right). Ten days after electrotransfer, ApN-KO mice were challenged by LPS, as described above.

The University Animal Care Committee approved all procedures.

Electrotransfer of ApN gene into muscle

Expression plasmids and DNA preparation

Plasmid pcDNA 3.1-ApN was constructed by inserting the mouse full-length ApN cDNA (19) into the *Kpn*I-*Age*I sites, between the cytomegalovirus promotor and a 3′ flanking sequence of bovine GH polyadenylation signal, in the pcDNA 3.1-V5-His A expression vector (Invitrogen, Life Technologies, Belgium). Plasmids were amplified in *E. coli* top 10 F′ (Invitrogen, Life Technologies, Merelbeke, Belgium), purified with an EndoFree plasmid giga kit (QIAGEN, Hilden, Germany), and then stocked at −80 C.

DNA injection and electroporation

Thirty microliters of plasmid solution (1 μg/μl) were injected into each tibialis anterior. Muscles were then electroporated by using transcutaneous electric pulses (eight square-wave pulses of 200 V/cm and 20 msec per pulse at 2 Hz) that were applied by two 4-mm spaced electrodes. Pulses were delivered by a Cliniporator system (IGEA, Carpi, Italy), as described (20, 21).

Quantification of circulating parameters

Blood glucose was measured using a glucometer (Medisense Precision Xtra Plus; Abott-Medisense, Louvain-la-Neuve, Belgium). Plasma was used for the other measurements. ApN, TNF-α, and nonesterified fatty acid (NEFA) concentrations were determined by commercially available kits (RIA mouse adiponectin kit; Linco Research, St. Charles, MO; ELISA mouse TNF-α kit, Biosource International, Inc., Camarillo, CA; Wako NEFA C kit; Wako Chemical GmbH, Neuss, Germany) as reported before (13). Lipid peroxidation was assessed by measuring plasma thiobarbituric acid reactive substance (TBARS) formation as described (22).

Light microscopy, immunohistochemistry, and morphometry

Muscle samples were fixed in 10% formaldehyde for 24 h and embedded in paraffin. Five-micrometer-thick sections were stained with hematoxylin-eosin-safran (HES). For immunohistochemistry, sections were processed as previously described (23) using rabbit polyclonal antibodies directed against ApN (Chemicon, Biognost, Heule, Belgium), caspase-6 (Tebu-bio, Baeckout, Belgium), peroxiredoxin (PRDX)-3, PRDX5 [gifts

from B. Knoops, University of Louvain, Brussels, Belgium (24)], 4-hydroxy-2-nonenal (HNE; Calbiochem, Damstadt, Germany), heme oxygenase 1 (HO-1) (Abcam, Cambridge, UK), TNF-α (Abcam), and NF-κB (Abcam). Antibody concentrations and incubation times were 1 μg/ml for 48 h (ApN), 10 μg/ml overnight (caspase-6, HO-1, TNF-α), 5 μg/ml overnight (PRDX3, HNE), 2 μg/ml overnight (PRDX5), and 20 μg/ml overnight (NF-κB). Sections used for ApN, caspase-6, HNE, HO-1, and NF-κB were pretreated in a microwave oven in Tris-citrate buffer (pH 6.5) for one cycle of 3 min at 750 W and three cycles of 3.5 min at 350 W. Binding of antibodies was detected by applying for 30 min at room temperature a second antibody, which was a goat antirabbit immunoglobulin conjugated to peroxidase-labeled polymer (En Vision +; Dako, Copenhagen, Denmark). Peroxidase activity was revealed with 3-amino-9-ethylcarbazole substrate (Dako, Copenhagen, Denmark), which produces a red stain. For quantification of caspase-6 and NF-κB, the percentage of immunolabeled nuclei was counted on magnification ×400. Immunohistochemical controls were performed by omission of the first antibody or the first and second antibodies, using preimmune serum, and incubation with an irrelevant antibody (antithyroglobulin).

Immunogold electron microscopy

Samples were fixed in 2.5% glutaraldehyde in 0.1 M cacodylate buffer for 1.5 h and embedded in LX112 resin (Ladd Research Industries, Burlington, VT). Ultrathin sections (0.1 μm) were rinsed in PBS-BSA 1% and incubated for 48 h with the rabbit polyclonal antiadiponectin antibody (10 μg/ml; Chemicon). Then they were rinsed and incubated for 30 min with a 15-nm colloidal gold affinity pure goat antirabbit IgG (Aurion, Wageningen, The Netherlands). Sections were postfixed with 2.5% glutaraldehyde for 5 min and counterstained. They were examined with a Zeiss 109 transmission electron microscope (Carl Zeiss, Oberkochem, Germany). Negative control was obtained by omission of primary antibody.

Cell culture

C2C12 myoblasts were cultured as previously described (12). Briefly, after proliferation, cells were cultured in basal medium (high glucose DMEM + 2% heat-inactivated horse serum) for 6 d to induce myogenic differentiation. Myotubes were used at this stage. Myotubes were then pretreated or not with 5 μg/ml mouse full-length recombinant ApN (Biovendor GmbH, Heidelberg, Germany) added to the basal medium for 18 h; these conditions were chosen according to a previous report (25) and our own preliminary data. Next, ultrapure LPS from *E. coli* K12 (Cayla-Invivogen Europe, Toulouse, France) was added for up to 4 h. At the end of the culture, cells were washed in ice-cold PBS before RNA or nuclear extraction.

RNA extraction and real-time quantitative PCR (RTQ-PCR)

RNA was isolated from mouse muscles and cultured cells with TriPure reagent (Roche Diagnostics, Vilvoorde, Belgium). Two micrograms of total RNA were reverse transcribed, as described previously (12). RTQ-PCR primers were designed (Primer Express Software; Applied Biosystems, Carlsbad, CA) for mouse AdipoR1, AdipoR2, ApN, cyclophilin, PRDX3, PRDX5, and TNF-α as reported (13, 26) and for HO-1 (sense, 5′-ACA GCA TGT CCC AGG ATT TGTC-3′; antisense, 3′-AAG GAG GCC ATC ACC AGC TT-5′), IL-6 (sense, 5′-TTC CAT CCA GTT GCC TTC TTG-3′; antisense, 3′-TTG GGA GTG GTA TCC TCT GTG-5′), and inhibitory-κB (IκB)-α (sense, 5′-TGG CCT TCC TCA ACT TCC AG-3′; antisense, 3′-GCA AGC TTT CAG AAG TGC CT-5′). Then 120 ng total RNA equivalents were amplified using an iCycler iQ real-time PCR detection system (Bio-Rad Laboratories, Nazareth, Belgium) (12). The threshold cycles (Ct) were measured in separate tubes and in duplicate. The identity and purity of the amplified product were checked by electrophoresis on agarose minigels, and analysis of the melting curve was carried out at the end of the amplification. To ensure the quality of the measurements, each plate included a negative control for each gene.

Nuclear extraction and measurement of NF-κB activity

After addition of hypotonic buffer (20 mM HEPES; 5.7 mM NaF; 1 mM EDTA, pH 7.5), C2C12 myotubes treated as described above were scraped with a cell lifter, transferred into a 1.5-ml tube, and placed on ice for 15 min. Nonidet P-40 (Sigma-Aldrich) was added to a final concentration of 0.5%, and the nuclei were pelleted by centrifugation (~250 × *g* for 4 min at 4 C). The nuclear pellet was resuspended in 50 μl Complete lysis buffer composed of AM1 lysis buffer (Active Motif Europe, Rixensart, Belgium), 1 mM dithiothreitol, and 1% protease inhibitor cocktail (Roche Diagnostics GmbH, Mannheim, Germany) and incubated for 15 min on ice with regular shacking, followed by a centrifugation (~1000 × *g* for 10 min at 4 C). Supernatants were collected and protein concentrations were determined by Bradford method.

Immunoreactive p65 binding to the NF-κB consensus DNA sequence was quantified in the nuclear extracts (6 μg protein) with a Trans-AM NF-κB transcription factor assay kit according to the manufacturer's instructions (Active Motive Europe).

Results presentation and statistical analysis

Results are means ± SEM. Ranges for gene expression levels were presented as $2^{-(\Delta\Delta Ct \pm SEM)}$, in which SEM is calculated from the ΔΔCt values (12).

Comparisons between two conditions (effects of electrotransfer with ApN plasmid *vs.* empty plasmid) were made using two-tailed paired Student's *t* test. Comparisons of three conditions (*in vitro* experiments) were carried out by one-way ANOVA followed by a Newman-Keuls test. When the four groups of mice were compared, the influence of genotype and that of treatment were assessed by two-way ANOVA followed by the *post hoc* Bonferroni test (Prism 4; GraphPad Software, San Diego, CA). Differences were considered statistically significant at $P < 0.05$.

Results

Body and tissue weights and circulating parameters of ApN-KO mice

As shown in Table 1, there were no significant differences in body weight and muscle weights between ApN-KO and WT mice receiving either LPS or saline (Table 1). However, inguinal fat pad weight was heavier in ApN-KO than WT

TABLE 1. Body weight, organ weights, and circulating parameters in the four groups of fasted mice

	WT	ApN-KO	WT + LPS	ApN-KO + LPS
Body weight (g)	23.6 ± 0.5	25.0 ± 1.0	22.4 ± 0.7	24.4 ± 0.6
Δ (g)	−3.7 ± 0.1	−3.6 ± 0.4	−3.3 ± 0.1	−3.1 ± 0.2
Tibialis anterior muscle				
Weight (mg)	92.9 ± 1.7	97.0 ± 3.9	84.9 ± 3.9	91.7 ± 2.3
Relative weight (mg/g)	0.39 ± 0.01	0.39 ± 0.01	0.38 ± 0.01	0.38 ± 0.01
Inguinal adipose tissue				
Weight (mg)	114.4 ± 0.5	207.3 ± 25.8[a]	119.6 ± 11.3	195.1 ± 13.9[a]
Relative weight (mg/g)	0.49 ± 0.04	0.83 ± 0.1[a]	0.53 ± 0.05	0.80 ± 0.05[b]
Circulating parameters				
Blood glucose (mg/liter)				
0 h	—	—	163 ± 5	156 ± 5
1 h after LPS	—	—	229 ± 7	216 ± 11
3 h after LPS	—	—	167 ± 6	156 ± 9
24 h after LPS	103 ± 4	105 ± 2	96 ± 6	95 ± 6
Plasma NEFAs (mg/dl)	71.2 ± 10.1	86.8 ± 13.1	77.0 ± 8.2	70.1 ± 9.0
Plasma TBARS (μmol/liter)	8.0 ± 1.8	7.5 ± 0.9	8.1 ± 0.6	9.7 ± 1.0
Plasma TNF-α (pg/ml)				
0 h	—	—	ND	ND
1 h after LPS	—	—	329 ± 19	300 ± 29
3 h after LPS	—	—	125 ± 12	82 ± 23
24 h after LPS	ND	ND	ND	ND
Plasma ApN (μg/ml)	7.9 ± 0.5	ND	5.8 ± 0.4[c]	ND

Four groups of mice were studied: untreated WT mice, untreated ApN-KO, LPS-treated wild-type mice (WT + LPS), and LPS-treated ApN-KO mice (ApN-KO + LPS). Treated mice received LPS injection and untreated mice were injected with vehicle only (saline). After the injection, mice from all groups were fasted for 24 h. Blood was obtained at the end of the study (24 h, unless otherwise indicated). Organ weights refer to pairs of muscles or fat pads, and relative organ weights are expressed as milligrams per gram body weight. Data are means ± SEM for six mice per group. Additional mice were used for measurements of glucose and TNF-α at 0, 1, and 3 h after LPS. Δ Body weight, Changes in weight over the 24 h of the study; ND, not detectable; −, not measured.

[a] $P < 0.01$ for the effect of genotype.

[b] $P < 0.05$ for the effect of genotype.

[c] $P < 0.01$ for the effect of treatment.

mice (Table 1), at variance with the original paper describing this strain (18), a finding that may perhaps be ascribed to differences in diet composition.

Blood was sampled 24 h after the injection of LPS/saline in fasted mice and also at intermediary time points when indicated. Glycemia peaked at 1 h after LPS and decreased thereafter to reach fasting values after 24 h. There were no differences in glycemia or plasma NEFAs between the different groups of mice. There were also no differences in plasma levels of TBARS, a marker of lipid peroxidation and systemic oxidative stress. The proinflammatory cytokine TNF-α was not detectable before and 24 h after LPS injection; the LPS-induced rise of TNF-α peaked at 1 h after the injection, concomitantly with the peak of glycemia that it could promote by inducing insulin resistance (2). This rise of TNFα was similar in ApN-KO and WT mice (Table 1). As expected, plasma ApN was undetectable in ApN-KO mice. WT mice treated by LPS displayed a moderate reduction of plasma ApN levels when compared with controls (Table 1), as already shown in rodents after polymicrobial sepsis (27).

Induction of ApN in the tibialis anterior of WT mice

Despite the decrease in circulating adiponectin, ApN was up-regulated in the skeletal muscle of WT mice challenged by LPS, in agreement with our previous work (12) (Fig. 1A). Thus, in saline-injected WT mice, there was only a very faint staining for ApN nearby the sarcolemma of muscle fibers, as already described (28) (Fig. 1A). By contrast, in LPS-injected WT mice, ApN was much more abundantly produced under the sarcolemma, whereas a faint labeling was also observed in the cytoplasm (Fig. 1A). ApN was not detectable in muscles of KO mice whether challenged or not by LPS (Fig. 1A).

The presence of ApN in skeletal muscle of WT mice was confirmed by immunogold detection in electron microscopy (Fig. 2). A few gold particles were detected in the muscular cells of control WT mice (Fig. 2B, *arrows*). In LPS-treated WT mice, ApN production was increased as indicated by the numerous gold particles in muscular cells. ApN was also abundantly detected in the extracellular space between two neighboring cells, thereby supporting the paradigm of a paracrine action of this myokine on muscle (Fig. 2C).

Evaluation of LPS-induced oxidative stress and inflammation in mouse muscles

To investigate the functional significance of muscular ApN expression in normal mice, we tested *a contrario* the hypothesis that skeletal muscle of ApN-KO mice would be more susceptible to inflammatory aggression. As assumed, the tibialis anterior muscle of ApN-KO mice ex-

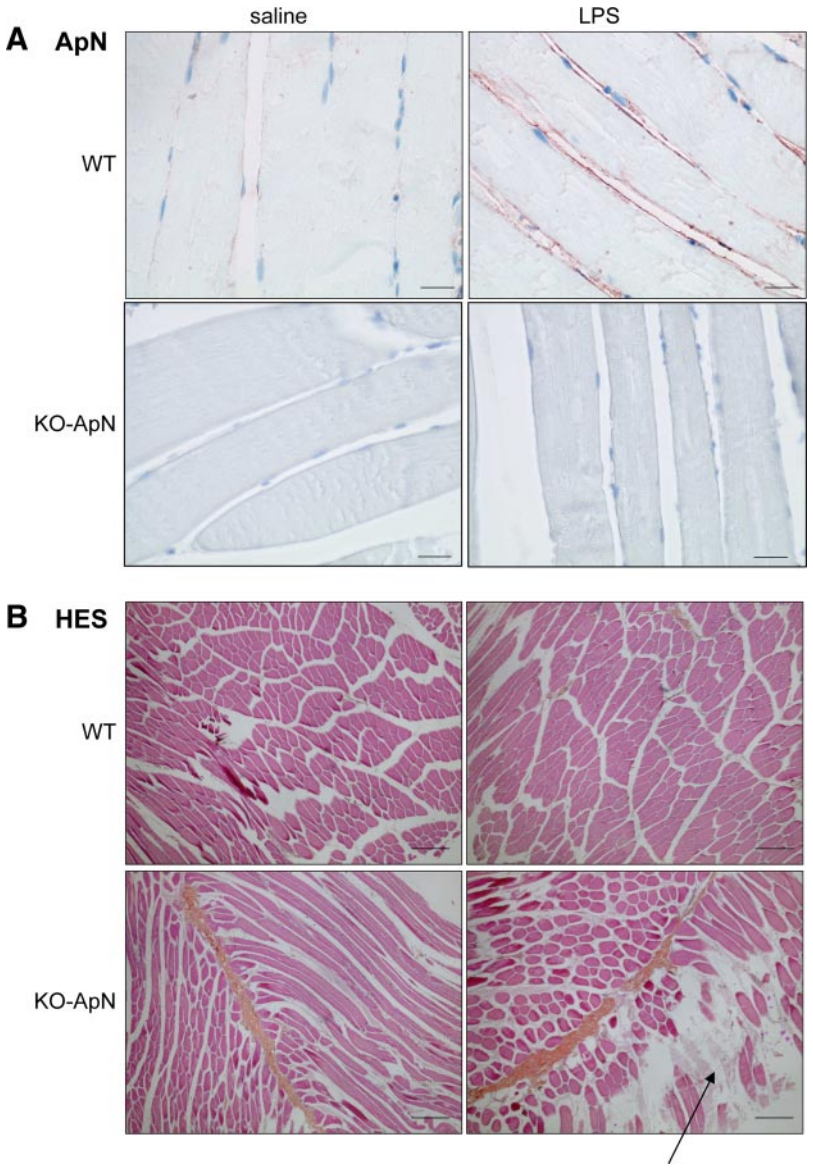

FIG. 1. Immunodetection of ApN production (A) and HES staining (B) in muscle sections of the four groups of mice. A, WT or ApN-KO mice were challenged by LPS (100 μg, ip), whereas other mice of each genotype received the vehicle (saline) only. Tibialis anterior muscles were sampled 24 h later. Myofibers of WT mice injected with LPS showed marked ApN labeling under the sarcolemma, compared with those receiving saline. There was no labeling in ApN-KO mice after either saline or LPS injection. *Scale bar*, 20 μm. B, HES staining in muscle sections of the four groups of mice. Tibialis anterior muscles were sampled as described above. Muscle sections of ApN-KO mice displayed degenerating myotubes mainly after LPS treatment (*arrow*). *Bar*, 100 μm. Representative sections for six mice per group are shown.

hibited some myocyte degeneration when compared with WT mice, especially after challenge by LPS (see Fig. 1B, HES coloration). Thus, muscle fibers were somewhat disorganized and ghost cells were present in these degenerating areas.

The mechanisms potentially involved in this degeneration were explored by searching for markers of oxidative stress, inflammation, and apoptosis.

In the basal state (*i.e.* saline administration), myotubes of ApN-KO mice already displayed enhanced expression of PRDX3 and PRDX5, two markers of oxidative stress, when compared with those of WT mice. After LPS injection, immunoreactivity for these proteins was also detectable in WT mice and was further increased in ApN-KO mice. Similar results were obtained for HO-1, another enzyme implicated in oxidative stress, for HNE, a lipid peroxidation product, and for TNF-α (Fig. 3, A and B). This up-regulation of TNFα in ApN-KO mice is in line with the concept that ApN and TNFα exert negative reciprocal interactions on their local production in some tissues (18, 26). The activation of caspase-6, an executioner caspase, which is up-regulated in several conditions of apoptosis in skeletal muscle (29–31), followed a similar pattern to that described above (Fig. 3, B and C). Thus, there was a slight activation of caspase-6, as shown by red nuclear labeling, in myofibers of ApN-KO mice studied in the basal state or in WT mice after LPS challenge (~10% of total nuclei). This immunoreactivity became much stronger in ApN-KO mice after LPS injection (~30% of total nuclei) (Fig. 3, B and C). Taken together, these data suggest that the degenerating cells, previously identified by HES staining in muscles of ApN-KO mice, were apoptotic as a consequence of the pronounced oxidative stress and inflammation.

In agreement with histochemistry analysis, muscular levels of PRDX3 mRNA were 2-fold higher in ApN-KO mice after LPS challenge than in similarly treated WT mice ($n = 6$ per group; $P < 0.05$). When compared with respective control (saline) mice, HO-1 mRNA abundance was 8- to 9-fold higher ($P < 0.01$) in mice of both genotypes after LPS. Likewise, LPS up-regulated TNF-α mRNAs in mice of both genotypes ($P < 0.01$) but to a greater extend in KO mice ($P < 0.05$) (relative expression to WT-saline: 13 ± 5 in WT-LPS and 40 ± 14 in KO-LPS). However, there were no significant differences between the two strains of mice studied in basal conditions (data not shown).

Effects of muscle electrotransfer of ApN gene on oxidative stress and inflammation in ApN-KO mice

In a second set of experiments, we directly tested the hypothesis that local administration of ApN could protect

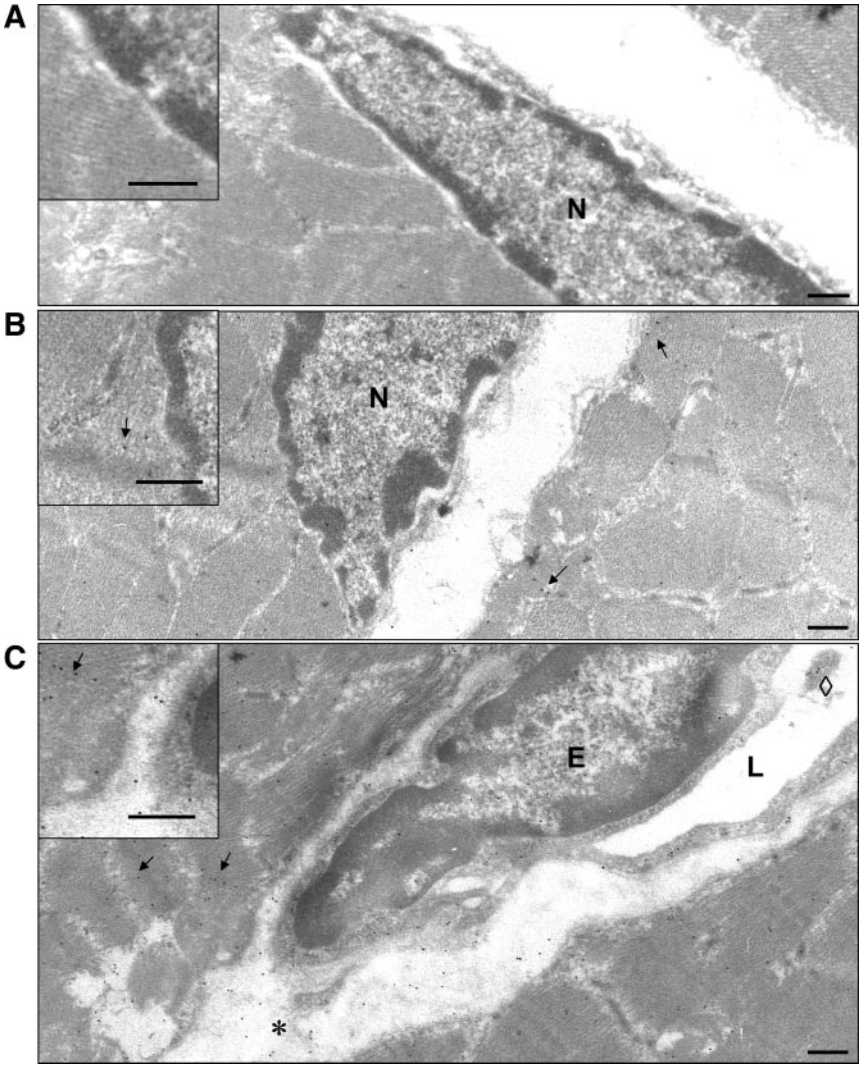

FIG. 2. Immunogold detection of ApN by electron microscopy in muscle sections of WT mice challenged or not by LPS. A, Specificity control by omission of the first antibody. No labeling was detected inside and outside the muscular cell. N, Nucleus. *Scale bar*, 1 μm. B, Control mouse receiving saline. A few gold particles were detected in the muscular cells (*arrows*). *Scale bar*, 1 μm. C, LPS-treated WT mouse. ApN production was increased as indicated by the numerous *gold particles* in muscular cells (*arrows*). ApN was released by the muscular cells and detected in the extracellular space (*star*) between two neighboring cells. A few *gold particles* were also observed in the lumen (L) of blood capillary (◊). E, Endothelial cell with its nucleus. *Scale bar*, 1 μm. *Inserts,* Magnification of the respective electron microscopy images. *Scale bars*, 1 μm.

ApN-KO mice against LPS-induced muscular damage. One tibialis anterior muscle was injected with a plasmid containing the ApN sequence and the contralateral muscle with an empty plasmid; muscles were then electroporated. Ten days later, mice were challenged by LPS. We found no difference in tissue weight between the two tibialis anterior muscles (not illustrated).

We first showed that electrotransfer of the ApN gene induced a local expression of ApN in the target muscle of ApN-KO mice (Fig. 4). Concomitantly, there was no expression of the adipokine in the contralateral muscle and no rise of ApN concentrations in the plasma, in which the levels remained undetectable (not shown).

Muscle electrotransfer of the *ApN* gene markedly reduced the expression of oxidative markers (PRDX3/5 and HO-1) when compared with the contralateral untreated muscle but also reduced that of the lipid peroxidation product (HNE), TNF-α, and caspase-6 (Fig. 4).

Potential involvement of NF-κB

NF-κB is a transcription factor that controls several genes involved in stress, inflammation, and apoptosis. Inhibition of this transcription factor in skeletal muscle exerts protective effects in models of muscle injury (32, 33). To attempt to identify the molecular pathways responsible for the protective effects of ApN, we thus measured NF-κB activation in our two sets of *in vivo* experiments.

In the first set of experiments, the percentage of NF-κB immunolabeled nuclei in myocytes was compared between the four groups of mice (ApN-KO and WT mice either saline or LPS injected). In the basal state, the percentage of NF-κB-immunolabeled nuclei was low in WT mice and was about 3-fold higher in ApN-KO mice (Fig. 5A). After LPS injection, the percentage of immunolabeled nuclei observed in WT mice was similar to the basal value of ApN-KO mice; this percentage further increased when ApN-KO mice were challenged by LPS, reaching up to 40% of total nuclei (Fig. 5A). These data are reminiscent of those obtained for caspase-6 (compare Figs. 5A and 3C).

In the second set of experiments dealing with electrotransfer, NF-κB activation was markedly reduced by muscular transfection of ApN in LPS-challenged KO mice. Thus, the percentage of labeled nuclei in the muscle transfected by the ApN cDNA-containing plasmid was approximately 3-fold lower than in the contralateral untreated muscle (Fig. 5, B and C).

Adiponectin prevention of LPS-induced proinflammatory cytokines and NF-κB transactivation in C2C12 myotubes

We examined whether pretreatment of myotubes with recombinant ApN could influence LPS-induced proinflammatory cytokine expression and transactivation of

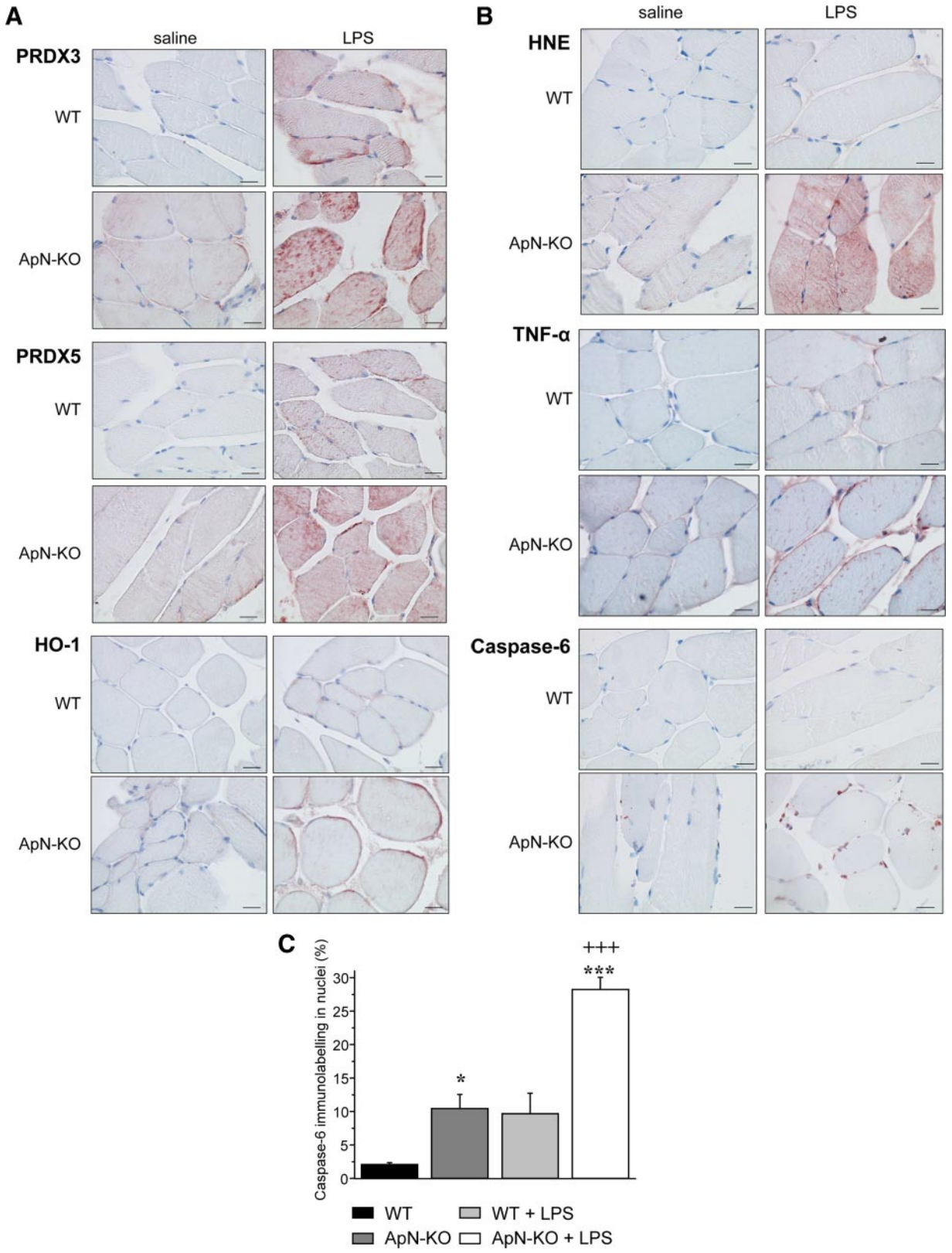

FIG. 3. Immunodetection of PDRX3/5, HO-1, HNE, TNF-α, and caspase-6 in muscle sections of the four groups of mice. Tibialis anterior muscles were sampled from ApN-KO and WT mice after saline or LPS treatment. Specific antibodies against PDRX3, PDRX5 and HO-1 (A) and HNE, TNF-α, and caspase-6 (B) were used. After saline (basal state), nuclear (caspase-6) and cytoplasmic labeling (other markers) was more pronounced in ApN-KO-mice than in WT mice. After LPS, some labeling was observed in WT mice, but immunoreactivity for all the studied markers was strikingly amplified in ApN-KO mice. Representative sections for six mice per group are shown. *Bar*, 20 μm. C, Quantification of caspase-6 immunolabeling in myofiber nuclei (expressed as percent total nuclei). Data are means $\pm$ SEM for six mice /group. *, $P < 0.05$, ***, $P < 0.001$ for the effect of genotype; +++, $P < 0.001$ for the effect of treatment.

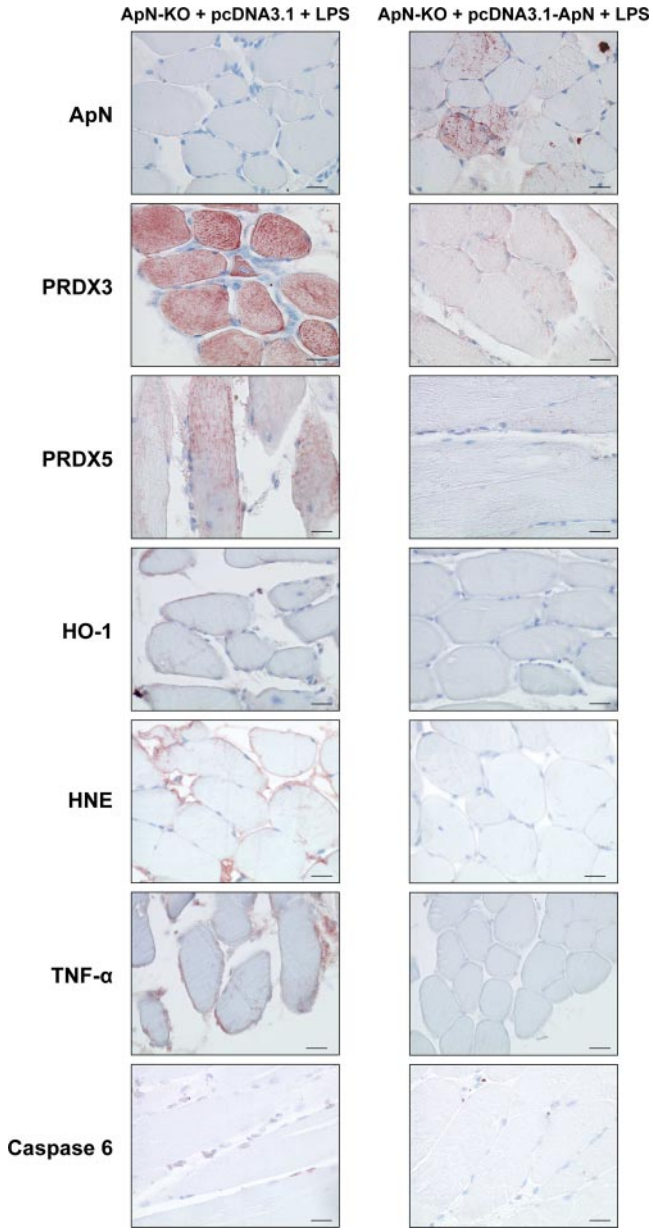

FIG. 4. Effects of ApN gene electrotransfer on ApN and stress marker expression in muscles of ApN-KO mice. One tibialis anterior muscle of ApN-KO mice was injected and electroporated with ApN cDNA-containing plasmid, whereas the contralateral muscle was injected and electroporated with a control plasmid. Ten days later, mice were challenged by LPS and the tibialis anterior muscles were sampled 24 h later. Immunodetection was performed as described above. ApN protein was detected in the muscle injected/electroporated with ApN cDNA, whereas no expression was detected in the muscle injected/electroporated with the control plasmid. Immunoreactivity for oxidative stress markers (PDRX3/5, HO-1, HNE), TNF-α, and caspase-6 was attenuated by ApN gene electrotransfer. *Bar*, 20 μm. Representative sections for three mice are shown.

NF-κB (Fig. 6). LPS increased gene expression of TNF-α, IL-6, and IκB-α in C2C12 myotubes. The quantification of IκB-α mRNAs, a target gene of NF-κB, is a sensitive method to quantify the transactivation of NF-κB (34). This transactivation was further confirmed by enhanced DNA-binding activity of NF-κB in nuclear extracts. The stimulatory effect of LPS on inflammation parameters and NF-κB activation was partially prevented by ApN pretreatment (Fig. 6).

It is of note that gene expression of ApN receptors, AdipoR1 and AdipoR2, in 6-d differentiated C2C12 cells was roughly similar to that observed in mouse tibialis anterior muscle with a greater (>1000-fold) mRNA abundance of AdipoR1 in both cases.

Discussion

We first confirmed our previous report that ApN may be induced in skeletal myocytes in response to LPS (12). We further showed that ApN exerts protective effects against an inflammatory aggression in muscle both *in vivo* and *in vitro*. When compared with WT mice, muscle of ApN-KO mice challenged by LPS displayed increased oxidative stress, inflammation, and apoptosis. Muscle transfer of the *ApN* gene via injection of ApN cDNA-containing plasmid followed by electroporation prevented all these abnormalities. Finally, *in vitro* ApN prevented LPS-induced production of proinflammatory cytokines in C2C12 myotubes. Taken together, these data suggest that the presence of ApN is crucial to counterbalance inflammatory aggression in mouse muscle. Yet this work is mainly based on a pharmacological approach, and further studies are needed to unequivocally assess the antiinflammatory and protective role of endogenous ApN in muscle.

Besides its antiatherogenic effects, ApN may exert antiinflammatory effects on other organs such as the liver, colon, or heart as shown by experiments using ApN-KO mice and/or systemic administration of the adipokine. Thus, ApN-KO mice developed more severe diet-induced steatohepatitis- or LPS-induced hepatotoxicity than WT mice (35–38), and systemic (ip or adenoviral mediated) administration of ApN prevented liver injury (36, 39). Likewise, ApN-KO mice developed much more severe chemically induced colitis than WT mice, whereas adenovirus-mediated supplementation of ApN significantly attenuated the severity of the disease (40). Yet contrasting data showing no effect of ApN on the liver and even an opposite (proinflammatory) effect on the colon have been reported in another strain of ApN-KO mice (41, 42). ApN may also exert cardioprotective effects. Thus, ischemia-reperfusion in ApN-KO mice resulted in increased myocardial infarct size, myocardial apoptosis, TNF-α expression, and reactive oxygen species/reactive nitrogen species production compared with WT mice (43, 44). Again, systemic administration of ApN rescued these abnormalities (43, 44). In all the studies mentioned above, the protective effect of ApN was demonstrated *in vivo* by using systemic supplementation of ApN, resulting in increased plasma

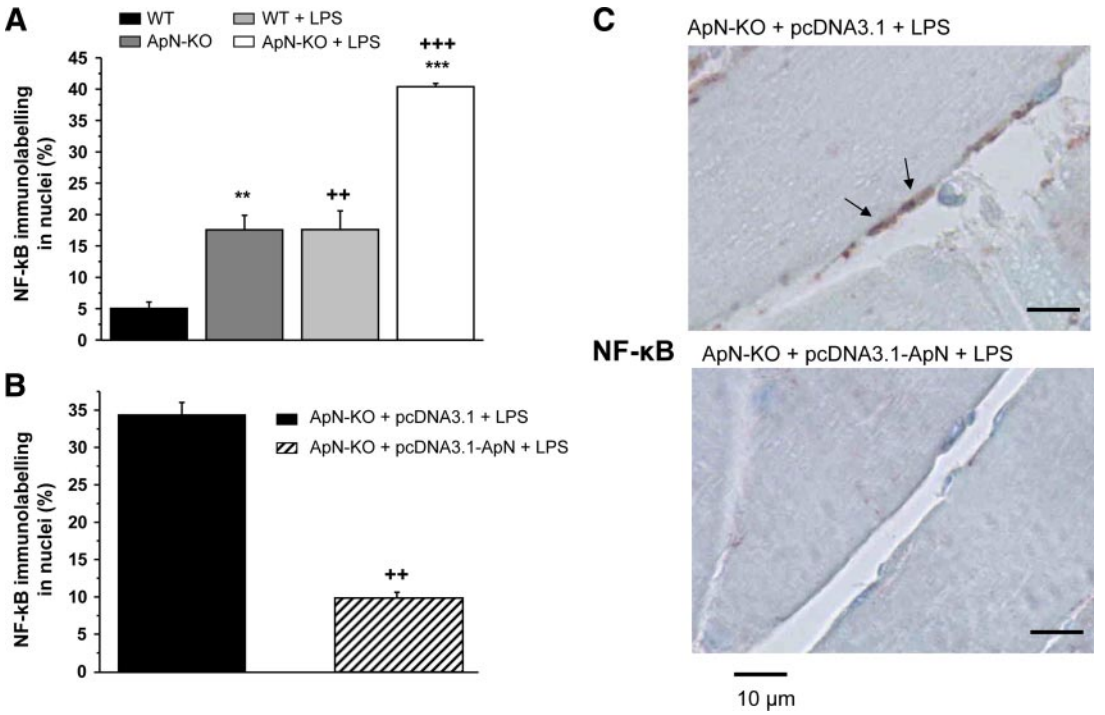

FIG. 5. Immunodetection of muscular NF-κB in the four groups of mice (A) or in ApN-KO mice after ApN gene electrotransfer (B and C). A and B, Quantification of nuclear NF-κB immunolabeling in muscles of the four groups of mice (A) or in muscles of ApN-KO mice transfected or not with the ApN gene before LPS challenge (B). Quantification was performed by analyzing sections as that shown in C. Data are means ± SEM for six mice/group (A) and for three mice [the contralateral muscle being used as control in this case (B)]. **, $P < 0.01$, ***, $P < 0.001$ for the effect of genotype; ++, $P < 0.01$, +++, $P < 0.001$ for the effect of treatment [LPS *vs.* saline (A) or electrotransfer of ApN cDNA containing-plasmid *vs.* empty plasmid (B)]. C, Nuclear labeling for the transcription factor NF-κB was attenuated by electrotransfer of the ApN gene in ApN-KO mice. *Bar*, 10 μm. Representative sections of three mice are shown. Positive (*red*) nuclei are indicated by *arrows*.

ApN levels. This rise in plasma ApN could be a confounding factor by affecting organs other than those studied so that the repercussions on the investigated tissue could be indirectly mediated. In the present work, muscle transfer of the *ApN* gene was not accompanied by any rise of circulating ApN. We therefore unambiguously show that the mere local restoration of ApN is sufficient to alleviate inflammation in skeletal muscle. This also suggests that ApN may exert some of its effects on muscle in an autocrine/paracrine manner, a paradigm further supported by immunogold labeling of ApN.

Unlike its metabolic effects that are reasonably well understood, the antiinflammatory effects of ApN involve a multiplicity of mechanisms that are still poorly defined and vary among its target tissues (1, 45, 46). In the cardiac muscle, ApN suppressed ischemia/reperfusion-induced TNF-α overproduction by up-regulating the cyclooxygenase-2-prostaglandin E_2-linked cascade (46). In the skeletal muscle, we found that ApN suppressed LPS-induced TNF-α overproduction and down-regulated NF-κB signaling. Thus, when compared with WT mice *in vivo*, the muscles of ApN-KO mice exhibited a higher degree of nuclear translocation of NF-κB after the LPS challenge, a finding attenuated by electrotransfer of the *ApN* gene. This did not result from changes in muscle gene expression of Toll-like receptor 4, the receptor for LPS (data not shown). Likewise, *in vitro*, ApN mitigated LPS-induced NF-κB activity and overexpression of proinflammatory cytokines in cultured C2C12 myotubes, thereby suggesting a direct antiinflammatory role of ApN on skeletal myocytes. Such a mechanism is in line with other studies performed *in vitro* in endothelial cells (7, 46, 47), macrophages (48, 49), or adipocytes (50) reporting that ApN may suppress NF-κB activation incited by LPS, TNF-α, or high glucose. Collectively, these and our own data may suggest that in skeletal muscle, the suppression by ApN of LPS-induced NF-κB activation reduces TNF-α, which in turn further contributes to attenuate NF-κB. Suppression of oxidative stress by ApN, as shown here in mouse muscle *in vivo* or in human and murine myotubes *in vitro* (51, 52), could contribute as well (53).

Besides protection against inflammation and oxidative stress, ApN up-regulation could also exert several other beneficial effects on muscle. First, ApN may supply extra fuel, which is needed to cope with a life-threatening situation. This is achieved because of the ability of ApN to stimulate glucose transport and fatty acid oxidation in skeletal muscle (54–56). Second, ApN may be viewed as a means to counteract muscle catabolism. ApN has been reported to block free fatty acid-induced muscle proteol-

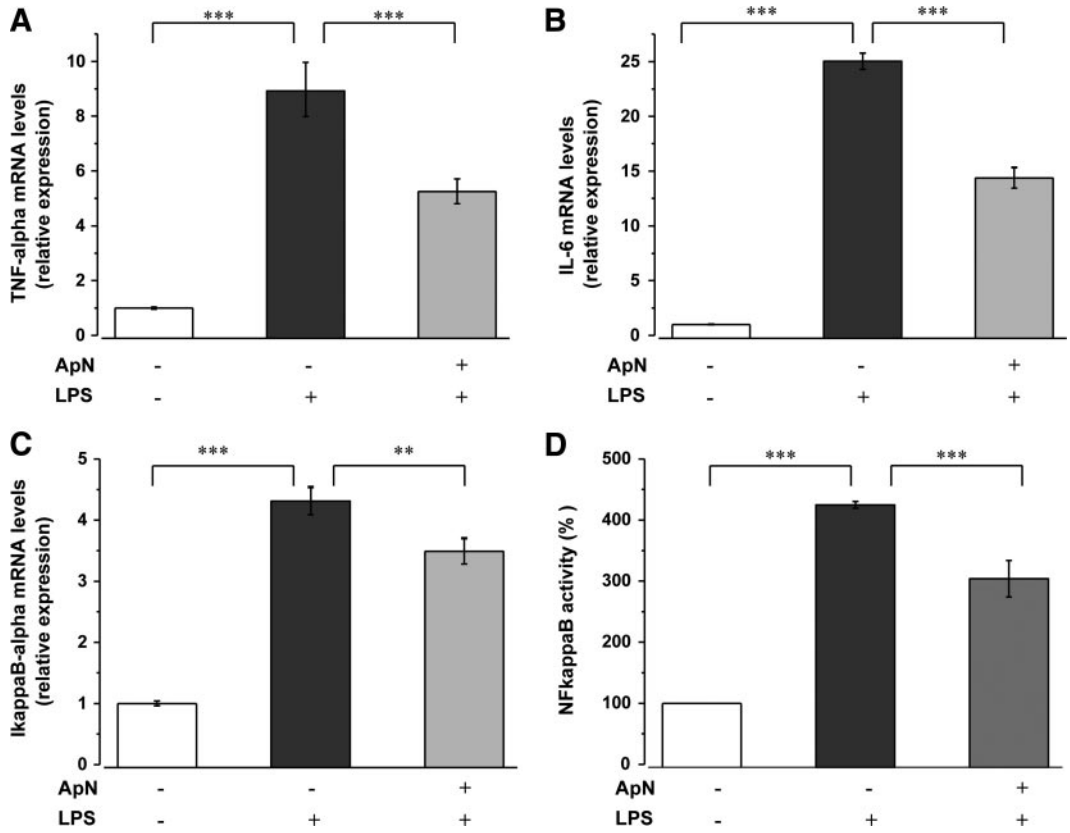

FIG. 6. ApN prevention of LPS-induced proinflammatory cytokine mRNAs and NF-κB activity in C2C12 myotubes. C2C12 myotubes were pretreated for 18 h with or without recombinant ApN (5 μg/ml) before the addition of LPS [1 μg/ml (A–C) or 33 ng/ml (D)] to this medium for another 4 h (A–C) or 3 h (D). mRNA levels of IL-6 (A), TNF-α (B), and IκB-α (C) were quantified by RTQ-PCR and are presented as relative expression compared with controls. Results are normalized to the level of cyclophilin and expressed as means ± SEM for 14 experiments. D, NF-κB (p65) DNA-binding activity was measured by ELISA in nuclear extracts. Results were calculated as OD units per 6 μg nuclear protein and then expressed as percentages of control values and presented as means ± SEM for nine experiments. **, $P < 0.01$; ***, $P < 0.001$.

ysis in C2C12 cells (57). However, in our electrotransfer experiments, when we compared the muscle transfected with the *ApN* gene with the control muscle, we did not find any changes in tibialis anterior weight (see *Results*) or in mRNA levels of atrogin-1 and muscle-specific ring finger protein-1, two ubiquitin ligases used as markers of proteolysis (57) (data not shown). Yet our experimental design was not maximized for this purpose, and these negative data do not exclude the possibility of an antiproteolytic effect of ApN. The tests were conducted in a limited number of mice (n = 4), and the time elapsed after LPS injection (24 h) might not have been optimal [a shorter time period (12 h) could have been more suitable for this aim; Jortay, J. and S. M. Brichard, unpublished time course data from WT mice]. Third, ApN may help to preserve muscle function and phenotype. Skeletal muscle of ApN-KO mice demonstrated impaired peak tetanic forces and increased fiber type IIb areas when compared with control mice. Thus, disruption of ApN may cause contractile dysfunction and phenotypical changes in skeletal muscle (15). Fourth, ApN may induce skeletal myogenesis. Globular ApN has been shown to induce *in vitro* the expression of specific skeletal muscle markers as well as provoke cell fusion into multinucleated syncytia and finally muscle fiber formation. These data put forward the possibility that ApN might contribute to skeletal muscle plasticity, potentially promoting the differentiation and fusion of myoblasts in the damaged muscles (58).

In conclusion, ApN exerts potent antiinflammatory, antioxidative, and antiapoptotic properties on skeletal muscle and concomitantly down-regulates NF-κB signaling. Therefore, ApN production, which is induced by skeletal muscle in response to inflammatory aggression, seems in turn to be crucial to locally counteract excessive and deleterious inflammatory/oxidative reactions.

Acknowledgments

We are grateful to Professor V. Préat for use of the electroporation system, C. de Ville de Goyet for electron microscopy experiments, and Drs. G. Vandermeulen and H. Gilson for help with mice electroporation and plasmid preparation, respectively.

Address all correspondence and requests for reprints to: S. M. Brichard, Unité d'Endocrinologie et Métabolisme, UCL/ENDO

5530, Avenue Hippocrate, 55, B-1200 Brussels, Belgium. E-mail: sonia.brichard@uclouvain.be.

This work was supported by Grant 3.4616.09 from the Foundation of Scientific and Medical Research and Grant ARC 05/10-328 from the General Division of Scientific Research. J.J. has a fellowship from the Fonds pour la Formation à la Recherche dans l'Industrie et l'Agriculture (Belgium).

Disclosure Summary: The authors have nothing to disclose.

References

1. **Ouchi N, Walsh K** 2007 Adiponectin as an anti-inflammatory factor. Clin Chim Acta 380:24–30
2. **Maury E, Brichard SM** 2010 Adipokine dysregulation, adipose tissue inflammation and metabolic syndrome. Mol Cell Endocrinol 314:1–16
3. **Guerre-Millo M** 2008 Adiponectin: an update. Diabetes Metab 34: 12–18
4. **Yamauchi T, Nio Y, Maki T, Kobayashi M, Takazawa T, Iwabu M, Okada-Iwabu M, Kawamoto S, Kubota N, Kubota T, Ito Y, Kamon J, Tsuchida A, Kumagai K, Kozono H, Hada Y, Ogata H, Tokuyama K, Tsunoda M, Ide T, Murakami K, Awazawa M, Takamoto I, Froguel P, Hara K, Tobe K, Nagai R, Ueki K, Kadowaki T** 2007 Targeted disruption of AdipoR1 and AdipoR2 causes abrogation of adiponectin binding and metabolic actions. Nat Med 13:332–339
5. **Yamauchi T, Kamon J, Ito Y, Tsuchida A, Yokomizo T, Kita S, Sugiyama T, Miyagishi M, Hara K, Tsunoda M, Murakami K, Ohteki T, Uchida S, Takekawa S, Waki H, Tsuno NH, Shibata Y, Terauchi Y, Froguel P, Tobe K, Koyasu S, Taira K, Kitamura T, Shimizu T, Nagai R, Kadowaki T** 2003 Cloning of adiponectin receptors that mediate antidiabetic metabolic effects. Nature 423: 762–769
6. **Kadowaki T, Yamauchi T, Kubota N, Hara K, Ueki K, Tobe K** 2006 Adiponectin and adiponectin receptors in insulin resistance, diabetes, and the metabolic syndrome. J Clin Invest 116:1784–1792
7. **Ouchi N, Kihara S, Arita Y, Okamoto Y, Maeda K, Kuriyama H, Hotta K, Nishida M, Takahashi M, Muraguchi M, Ohmoto Y, Nakamura T, Yamashita S, Funahashi T, Matsuzawa Y** 2000 Adiponectin, an adipocyte-derived plasma protein, inhibits endothelial NF-κB signaling through a cAMP-dependent pathway. Circulation 102:1296–1301
8. **Motoshima H, Wu X, Mahadev K, Goldstein BJ** 2004 Adiponectin suppresses proliferation and superoxide generation and enhances eNOS activity in endothelial cells treated with oxidized LDL. Biochem Biophys Res Commun 315:264–271
9. **Satoh N, Naruse M, Usui T, Tagami T, Suganami T, Yamada K, Kuzuya H, Shimatsu A, Ogawa Y** 2004 Leptin-to-adiponectin ratio as a potential atherogenic index in obese type 2 diabetic patients. Diabetes Care 27:2488–2490
10. **Pedersen BK, Febbraio MA** 2008 Muscle as an endocrine organ: focus on muscle-derived interleukin-6. Physiol Rev 88:1379–1406
11. **Staiger H, Kausch C, Guirguis A, Weisser M, Maerker E, Stumvoll M, Lammers R, Machicao F, Häring HU** 2003 Induction of adiponectin gene expression in human myotubes by an adiponectin-containing HEK293 cell culture supernatant. Diabetologia 46: 956–960
12. **Delaigle AM, Jonas JC, Bauche IB, Cornu O, Brichard SM** 2004 Induction of adiponectin in skeletal muscle by inflammatory cytokines: *in vivo* and *in vitro* studies. Endocrinology 145:5589–5597
13. **Delaigle AM, Senou M, Guiot Y, Many MC, Brichard SM** 2006 Induction of adiponectin in skeletal muscle of type 2 diabetic mice: *in vivo* and *in vitro* studies. Diabetologia 49:1311–1323
14. **Yang B, Chen L, Qian Y, Triantafillou JA, McNulty JA, Carrick K, Clifton LG, Han B, Geske R, Strum J, Brown KK, Stimpson SA, Pahel G** 2006 Changes of skeletal muscle adiponectin content in diet-induced insulin resistant rats. Biochem Biophys Res Commun 341:209–217
15. **Krause MP, Liu Y, Vu V, Chan L, Xu A, Riddell MC, Sweeney G, Hawke TJ** 2008 Adiponectin is expressed by skeletal muscle fibers and influences muscle phenotype and function. Am J Physiol Cell Physiol 295:C203–C212
16. **Liu Y, Chewchuk S, Lavigne C, Brûlé S, Pilon G, Houde V, Xu A, Marette A, Sweeney G** 2009 Functional significance of skeletal muscle adiponectin production, changes in animal models of obesity and diabetes, and regulation by rosiglitazone treatment. Am J Physiol Endocrinol Metab 297:E657–E664
17. **Bonnard C, Durand A, Vidal H, Rieusset J** 2008 Changes in adiponectin, its receptors and AMPK activity in tissues of diet-induced diabetic mice. Diabetes Metab 34:52–61
18. **Maeda N, Shimomura I, Kishida K, Nishizawa H, Matsuda M, Nagaretani H, Furuyama N, Kondo H, Takahashi M, Arita Y, Komuro R, Ouchi N, Kihara S, Tochino Y, Okutomi K, Horie M, Takeda S, Aoyama T, Funahashi T, Matsuzawa Y** 2002 Diet-induced insulin resistance in mice lacking adiponectin/ACRP30. Nat Med 8:731–737
19. **Bauche IB, Ait El Mkadem S, Rezsohazy R, Funahashi T, Maeda N, Miranda LM, Brichard SM** 2006 Adiponectin down-regulates its own production and the expression of its AdipoR2 receptor in transgenic mice. Biochem Biophys Res Commun 345:1414–1424
20. **Vandermeulen G, Staes E, Vanderhaeghen ML, Bureau MF, Scherman D, Préat V** 2007 Optimisation of intradermal DNA electrotransfer for immunisation. J Control Release 124:81–87
21. **Gilson H, Schakman O, Kalista S, Lause P, Tsuchida K, Thissen JP** 2009 Follistatin induces muscle hypertrophy through satellite cell proliferation and inhibition of both myostatin and activin. Am J Physiol Endocrinol Metab 297:E157–E164
22. **Scoccia AE, Molinuevo MS, McCarthy AD, Cortizo AM** 2001 A simple method to assess the oxidative susceptibility of low density lipoproteins. BMC Clin Pathol 1:1
23. **Gérard AC, Many MC, Daumerie C, Costagliola S, Miot F, DeVijlder JJ, Colin IM, Denef JF** 2002 Structural changes in the angiofollicular units between active and hypofunctioning follicles align with differences in the epithelial expression of newly discovered proteins involved in iodine transport and organification. J Clin Endocrinol Metab 87:1291–1299
24. **Leyens G, Donnay I, Knoops B** 2003 Cloning of bovine peroxiredoxins-gene expression in bovine tissues and amino acid sequence comparison with rat, mouse and primate peroxiredoxins. Comp Biochem Physiol B Biochem Mol Biol 136:943–955
25. **Haugen F, Drevon CA** 2007 Activation of nuclear factor-κB by high molecular weight and globular adiponectin. Endocrinology 148: 5478–5486
26. **Bauche IB, El Mkadem SA, Pottier AM, Senou M, Many MC, Rezsohazy R, Penicaud L, Maeda N, Funahashi T, Brichard SM** 2007 Overexpression of adiponectin targeted to adipose tissue in transgenic mice: impaired adipocyte differentiation. Endocrinology 148:1539–1549
27. **Tsuchihashi H, Yamamoto H, Maeda K, Ugi S, Mori T, Shimizu T, Endo Y, Hanasawa K, Tani T** 2006 Circulating concentrations of adiponectin, an endogenous lipopolysaccharide neutralizing protein, decrease in rats with polymicrobial sepsis. J Surg Res 134: 348–353
28. **Punyadeera C, Zorenc AH, Koopman R, McAinch AJ, Smit E, Manders R, Keizer HA, Cameron-Smith D, van Loon LJ** 2005 The effects of exercise and adipose tissue lipolysis on plasma adiponectin concentration and adiponectin receptor expression in human skeletal muscle. Eur J Endocrinol 152:427–436
29. **Singh AB, Kaushal V, Megyesi JK, Shah SV, Kaushal GP** 2002 Cloning and expression of rat caspase-6 and its localization in renal ischemia/reperfusion injury. Kidney Int 62:106–115
30. **Belizário JE, Lorite MJ, Tisdale MJ** 2001 Cleavage of caspases-1, -3, -6, -8 and -9 substrates by proteases in skeletal muscles from mice undergoing cancer cachexia. Br J Cancer 84:1135–1140

31. **Tews DS** 2006 Characterization of initiator and effector caspase expressions in dystrophinopathies. Neuropathology 26:24–31
32. **Mourkioti F, Kratsios P, Luedde T, Song YH, Delafontaine P, Adami R, Parente V, Bottinelli R, Pasparakis M, Rosenthal N** 2006 Targeted ablation of IKK2 improves skeletal muscle strength, maintains mass, and promotes regeneration. J Clin Invest 116:2945–2954
33. **Acharyya S, Villalta SA, Bakkar N, Bupha-Intr T, Janssen PM, Carathers M, Li ZW, Beg AA, Ghosh S, Sahenk Z, Weinstein M, Gardner KL, Rafael-Fortney JA, Karin M, Tidball JG, Baldwin AS, Guttridge DC** 2007 Interplay of IKK/NF-κB signaling in macrophages and myofibers promotes muscle degeneration in Duchenne muscular dystrophy. J Clin Invest 117:889–901
34. **Bottero V, Imbert V, Frelin C, Formento JL, Peyron JF** 2003 Monitoring NF-κB transactivation potential via real-time PCR quantification of IκB-α gene expression. Mol Diagn 7:187–194
35. **Matsumoto H, Tamura S, Kamada Y, Kiso S, Fukushima J, Wada A, Maeda N, Kihara S, Funahashi T, Matsuzawa Y, Shimomura I, Hayashi N** 2006 Adiponectin deficiency exacerbates lipopolysaccharide/D-galactosamine-induced liver injury in mice. World J Gastroenterol 12:3352–3358
36. **Kamada Y, Matsumoto H, Tamura S, Fukushima J, Kiso S, Fukui K, Igura T, Maeda N, Kihara S, Funahashi T, Matsuzawa Y, Shimomura I, Hayashi N** 2007 Hypoadiponectinemia accelerates hepatic tumor formation in a nonalcoholic steatohepatitis mouse model. J Hepatol 47:556–564
37. **Asano T, Watanabe K, Kubota N, Gunji T, Omata M, Kadowaki T, Ohnishi S** 2009 Adiponectin knockout mice on high fat diet develop fibrosing steatohepatitis. J Gastroenterol Hepatol 24:1669–1676
38. **Uji Y, Yamamoto H, Tsuchihashi H, Maeda K, Funahashi T, Shimomura I, Shimizu T, Endo Y, Tani T** 2009 Adiponectin deficiency is associated with severe polymicrobial sepsis, high inflammatory cytokine levels, and high mortality. Surgery 145:550–557
39. **Masaki T, Chiba S, Tatsukawa H, Yasuda T, Noguchi H, Seike M, Yoshimatsu H** 2004 Adiponectin protects LPS-induced liver injury through modulation of TNF-α in KK-Ay obese mice. Hepatology 40:177–184
40. **Nishihara T, Matsuda M, Araki H, Oshima K, Kihara S, Funahashi T, Shimomura I** 2006 Effect of adiponectin on murine colitis induced by dextran sulfate sodium. Gastroenterology 131:853–861
41. **Pini M, Sennello JA, Chan L, Fantuzzi G** 2006 Adiponectin deficiency does not affect the inflammatory response to endotoxin or concanavalin a in mice. Endocrinology 147:5019–5022
42. **Fayad R, Pini M, Sennello JA, Cabay RJ, Chan L, Xu A, Fantuzzi G** 2007 Adiponectin deficiency protects mice from chemically induced colonic inflammation. Gastroenterology 132:601–614
43. **Shibata R, Sato K, Pimentel DR, Takemura Y, Kihara S, Ohashi K, Funahashi T, Ouchi N, Walsh K** 2005 Adiponectin protects against myocardial ischemia-reperfusion injury through. Nat Med 11:1096–1103
44. **Tao L, Gao E, Jiao X, Yuan Y, Li S, Christopher TA, Lopez BL, Koch W, Chan L, Goldstein BJ, Ma XL** 2007 Adiponectin cardioprotection after myocardial ischemia/reperfusion involves the reduction of oxidative/nitrative stress. Circulation 115:1408–1416
45. **Ouchi N, Walsh K** 2008 A novel role for adiponectin in the regulation of inflammation. Arterioscler Thromb Vasc Biol 28:1219–1221
46. **Goldstein BJ, Scalia RG, Ma XL** 2009 Protective vascular and myocardial effects of adiponectin. Nat Clin Pract Cardiovasc Med 6:27–35
47. **Devaraj S, Torok N, Dasu MR, Samols D, Jialal I** 2008 Adiponectin decreases C-reactive protein synthesis and secretion from endothelial cells: evidence for an adipose tissue-vascular loop. Arterioscler Thromb Vasc Biol 28:1368–1374
48. **Yokota T, Oritani K, Takahashi I, Ishikawa J, Matsuyama A, Ouchi N, Kihara S, Funahashi T, Tenner AJ, Tomiyama Y, Matsuzawa Y** 2000 Adiponectin, a new member of the family of soluble defense collagens, negatively regulates the growth of myelomonocytic progenitors and the functions of macrophages. Blood 96:1723–1732
49. **Yamaguchi N, Argueta JG, Masuhiro Y, Kagishita M, Nonaka K, Saito T, Hanazawa S, Yamashita Y** 2005 Adiponectin inhibits Toll-like receptor family-induced signaling. FEBS Lett 579:6821–6826
50. **Ajuwon KM, Spurlock ME** 2005 Adiponectin inhibits LPS-induced NF-κB activation and IL-6 production and increases PPARγ2 expression in adipocytes. Am J Physiol Regul Integr Comp Physiol 288:R1220–R1225
51. **Civitarese AE, Ukropcova B, Carling S, Hulver M, DeFronzo RA, Mandarino L, Ravussin E, Smith SR** 2006 Role of adiponectin in human skeletal muscle bioenergetics. Cell Metab 4:75–87
52. **Ikegami Y, Inukai K, Imai K, Sakamoto Y, Katagiri H, Kurihara S, Awata T, Katayama S** 2009 Adiponectin up-regulates ferritin heavy chain in skeletal muscle cells. Diabetes 58:61–70
53. **Silveira LR, Fiamoncini J, Hirabara SM, Procópio J, Cambiaghi TD, Pinheiro CH, Lopes LR, Curi R** 2008 Updating the effects of fatty acids on skeletal muscle. J Cell Physiol 217:1–12
54. **Fruebis J, Tsao TS, Javorschi S, Ebbets-Reed D, Erickson MR, Yen FT, Bihain BE, Lodish HF** 2001 Proteolytic cleavage product of 30-kDa adipocyte complement-related protein increases fatty acid oxidation in muscle and causes weight loss in mice. Proc Natl Acad Sci USA 98:2005–2010
55. **Tomas E, Tsao TS, Saha AK, Murrey HE, Zhang Cc, Itani SI, Lodish HF, Ruderman NB** 2002 Enhanced muscle fat oxidation and glucose transport by ACRP30 globular domain: acetyl-CoA carboxylase inhibition and AMP-activated protein kinase activation. Proc Natl Acad Sci USA 99:16309–16313
56. **Yamauchi T, Kamon J, Minokoshi Y, Ito Y, Waki H, Uchida S, Yamashita S, Noda M, Kita S, Ueki K, Eto K, Akanuma Y, Froguel P, Foufelle F, Ferre P, Carling D, Kimura S, Nagai R, Kahn BB, Kadowaki T** 2002 Adiponectin stimulates glucose utilization and fatty-acid oxidation by activating AMP-activated protein kinase. Nat Med 8:1288–1295
57. **Zhou Q, Du J, Hu Z, Walsh K, Wang XH** 2007 Evidence for adipose-muscle cross talk: opposing regulation of muscle proteolysis by adiponectin and fatty acids. Endocrinology 148:5696–5705
58. **Fiaschi T, Cirelli D, Comito G, Gelmini S, Ramponi G, Serio M, Chiarugi P** 2009 Globular adiponectin induces differentiation and fusion of skeletal muscle cells. Cell Res 19:584–597